JNM

PET and the Autoradiographic Method with Continuous Inhalation of Oxygen-15-Gas: Theoretical Analysis and Comparison with Conventional Steady-State Methods

Norihiro Sadato, Yoshiharu Yonekura, Michio Senda, Yasushi Iwasaki, Naoki Matoba, Nagara Tamaki, Satoshi Sasayama, Yasuhiro Magata and Junji Konishi

Reprinted from The Journal of Nuclear Medicine • Vol. 34 • No. 10 • October 1993

PET and the Autoradiographic Method with Continuous Inhalation of Oxygen-15-Gas: Theoretical Analysis and Comparison with Conventional Steady-State Methods

Norihiro Sadato, Yoshiharu Yonekura, Michio Senda, Yasushi Iwasaki, Naoki Matoba, Nagara Tamaki, Satoshi Sasayama, Yasuhiro Magata and Junji Konishi

Departments of Nuclear Medicine and Brain Pathophysiology, Kyoto University Faculty of Medicine, Kyoto, Japan; and Tokyo Metropolitan Institute of Gerontology, Tokyo, Japan

The steady-state method using ^{15}O gas inhalation and positron emission tomography (PET) is a simple and practical way of imaging cerebral blood flow (CBF) and oxygen metabolism. Several disadvantages do exist, however, including prolonged examination time, requirement of steady-state and a large tissue heterogeneity effect. To avoid the drawbacks of the steady-state method but to preserve its simplicity, we applied the PET/autoradiographic method to the build-up phase during the continuous inhalation of ^{15}O-gas with intermittent arterial sampling. A simulation study was performed to determine the optimal scanning period, evaluate the delay and dispersion effect of the input function and estimate the tissue heterogeneity effect. To assess the clinical feasibility of the proposed technique for the study of oxygen metabolism, sequential measurements with this method and the conventional steady-state method were performed in eight patients. The simulation study showed that a 5-min scan started 3 min after the commencement of ^{15}O-gas inhalation was optimal. With this method, the delay and dispersion effect on CBF was the same as that of the conventional steady-state method, but the tissue heterogeneity effect was reduced. In eight patients, CBF values calculated by this method showed time dependency and were slightly higher than those obtained by the steady-state method. The oxygen extraction fraction showed no significant time dependency and was well correlated with that obtained by the steady-state method. We conclude that the proposed method is a simple and acceptable alternative to the conventional steady-state method.

J Nucl Med 1993; 34:1672–1680

The continuous inhalation of ^{15}O-labeled CO_2 and O_2 (steady-state method) is widely used as a simple and practical method to measure regional cerebral blood flow (CBF), oxygen extraction fraction (OEF) and cerebral metabolic rate of oxygen consumption ($CMRO_2$) by positron emission tomography (PET) (*1*). The method, however, has several disadvantages (*2–5*). The relatively long inhalation period required to achieve steady state (approximately 8–10 min) exposes subjects to a high level of radiation and it is difficult to determine the exact time when the tracer concentration has reached the steady-state. Fluctuation of the arterial activity may lead to substantial error in the calculated values, which cannot be completely corrected by averaging techniques (*2*). Finally, the steady-state method is subject to the effect of tissue heterogeneity (*5–7*).

The examination time was shortened by the introduction of an autoradiographic method directly based on Kety's one-compartment model (*8*) without assuming steady-state (*6,9,10*). Recently, a combination of dynamic and autoradiographic methods was also applied in $C^{15}O_2$ inhalation studies (*11–13*). These methods are less affected by tissue heterogeneity, but are more affected by delay and dispersion problems (*11,12,14*). Rapid separation of plasma is also required for calculation of the OEF (*10*).

Senda et al. (*2*) applied the autoradiographic method to correct the variation in arterial radioactivity concentration in the near steady-state. Compared with the conventional steady-state method, this method can provide more robust parameters despite fluctuation of the arterial input function. However, it has the same disadvantages as the conventional method, that is, prolonged examination time and tissue heterogeneity effect. Because the algorithm of their method was similar to that used in the bolus injection of $H_2^{15}O$, it is applicable to the earlier phases in the gas inhalation method, resulting in faster examination and efficient use of the administered radiation dose. Considering the longer build-up phase during continuous inhalation of gas than during bolus administration, a reasonable compromise between accuracy of the parameters and simplicity of the procedure would seem to be possible.

The purpose of this study was to apply the autoradiographic method to the build-up phase while preserving the simplicity of the steady-state method.

Received Sept. 28, 1992; revision accepted Mar. 19, 1993.
For correspondence or reprints contact: Norihiro Sadato, MD, Rm. 5N226, Bldg. 10, National Institute of Neurological Disorders and Stroke, Bethesda, MD 20892.

MATERIALS AND METHODS

Formulas for Calculation

Formulas of the new method and the steady-state method are described in the Appendix.

CBF Measurement with $C^{15}O_2$ Inhalation

The regional change in cerebral radiotracer concentration during $C^{15}O_2$ inhalation is described as:

$$\frac{dC_T(t)}{dt} = FC_a(t) - \frac{FC_T(t)}{p} - \lambda C_T(t) = FC_a(t) - \left(\frac{F}{p} + \lambda\right)C_T(t),$$

where $C_T(t)$ is the tissue concentration of $H_2{}^{15}O$, $C_a(t)$ is the arterial concentration of $H_2{}^{15}O$, F is the regional blood flow, p is the partition coefficient of water between brain and blood (assumed as unity in this study), and λ is the physical decay constant of ^{15}O.

In steady-state, where $dC_T(t)/dt = 0$,

$$F = \frac{\lambda}{\frac{C_a}{C_T} \oplu \frac{1}{p}}.$$

In this method, the PET value T from t_1 to t_2 is:

$$T = \frac{1}{t_2 - t_1}\int_{t_1}^{t_2} k_1 C_a(t) * e^{-k_2 t}\, dt,$$

where * indicates convolution,

$$k_1 = F,$$

$$k_2 = \frac{F}{p} + \lambda,$$

assuming $C_T(t) = 0$.

This equation can be used to generate a lookup table, $F = G(T)$, that relates T to F, from which CBF is estimated.

OEF Measurement With $^{15}O_2$ Inhalation

The regional change in cerebral parenchymal radiotracer concentration during $^{15}O_2$ inhalation is:

$$\frac{dC_t(t)}{dt} = FEC_O(t) + FC_H(t) - \left(\frac{F}{p} + \lambda\right)C_t(t),$$

where E is the oxygen extraction fraction (OEF), $C_O(t)$ is the arterial concentration of $^{15}O_2$, and $C_H(t)$ is the arterial concentration of $H_2{}^{15}O$. In steady-state,

$$E = \frac{C_T\left(\frac{F}{p} + \lambda\right) - FC_H - V_b C_O\left(\frac{F}{p} + \lambda\right)}{pC_O - V_b C_O\left(\frac{F}{p} + \lambda\right)},$$

where V_b is the regional blood volume. In the new method,

$$E = \frac{\hat{C}_T - (C_1 + C_3)}{C_2 - C_1},$$

where $\hat{C}_T$ is PET value from t_1 to t_2,

$$C_1 = \frac{1}{t_2 - t_1}\int_{t_1}^{t_2} V_b C_O(t)\, dt$$

$$C_2 = \frac{1}{t_2 - t_1}\int_{t_1}^{t_2} FC_O(t) * e^{-k_2 t}\, dt$$

$$C_3 = \frac{1}{t_2 - t_1}\int_{t_1}^{t_2} FC_H(t) * e^{-k_2 t}\, dt.$$

Tomograph Characteristics

The PCT-3600W system (Hitachi Medical Co., Tokyo, Japan) was employed for PET scanning (*15,16*). This system simultaneously acquires 15 slices with a center-to-center distance of 7 mm. All scans were performed at a resolution of 9 mm full width at half maximum (FWHM) in the transaxial direction and 6.5 mm in the axial direction. Field of view and pixel size of the reconstructed images were 256 mm and 2 mm, respectively. A transmission scan was obtained before all emission measurements.

Subjects

We studied eight patients (age: 45–70 yr) who had cerebral infarction (six patients), Alzheimer type dementia (two patients), Binswanger's disease (one patient) and epilepsy (one patient). Informed consent was obtained from each subject using forms and procedures approved by the Ethical Committee of the Kyoto University Faculty of Medicine. The subject's head was immobilized with head holders. A small catheter was placed in the brachial artery for blood sampling. The subject wore a light, disposable, plastic mask and a nasal cannula through which he breathed $C^{15}O$, $C^{15}O_2$ and $^{15}O_2$ produced by a small cyclotron (CYPRIS model 325; Sumitomo Heavy Industries, Tokyo, Japan).

Tracer Techniques

CBV Study. To obtain the fractional regional cerebral blood volume (CBV), bolus inhalation of $C^{15}O$ with 3-min scanning was performed. Arterial samples were obtained manually twice during the scanning for calculation of CBV using the following formula:

$$CBV = \frac{PET}{RD\bar{C}_A} \times 100,$$

where PET is the PET value, $\bar{C}_A$ is the mean of the decay-corrected radiotracer concentration in arterial blood, R is the mean ratio of the small-vessel-to-large-vessel hematocrit, equal to 0.85 and D is the density of brain tissue, equal to 1.05 g/ml (*10*).

CBF and OEF Study. The subjects inhaled a steady supply of tracer amounts of $^{15}O_2$ for 18 min (Fig. 1). Scanning was started simultaneously with the commencement of $^{15}O_2$ inhalation. Dynamic scans of 18 consecutive frames (1 frame/min) were obtained. After a 15-min intermission, $C^{15}O_2$ was inhaled for 18 min for more dynamic scans with the same protocol.

Arterial blood was sampled manually from the brachial artery at 20 sec, 40 sec, 60 sec, 2 min, 4 min, 6 min, 8 min, 10 min, 12 min, 14 min, 16 min and 18 min after the commencement of inhalation. Each sample was collected for 10–20 sec to average the fluctuations due to the respiratory cycle (*2,17*), and activity of radiotracer concentrations in whole blood and plasma was measured with a well counter. Arterial hematocrit, PaO_2, $PaCO_2$, and arterial hemoglobin were also measured.

Data Processing

The arterial activity curves were determined with interpolation between the measured points. The reconstructed dynamic images of frames 5–8 and 9–13 were added to make the late build-up phase images and near steady-state images, respectively. For the conventional steady-state method, near steady-state images and

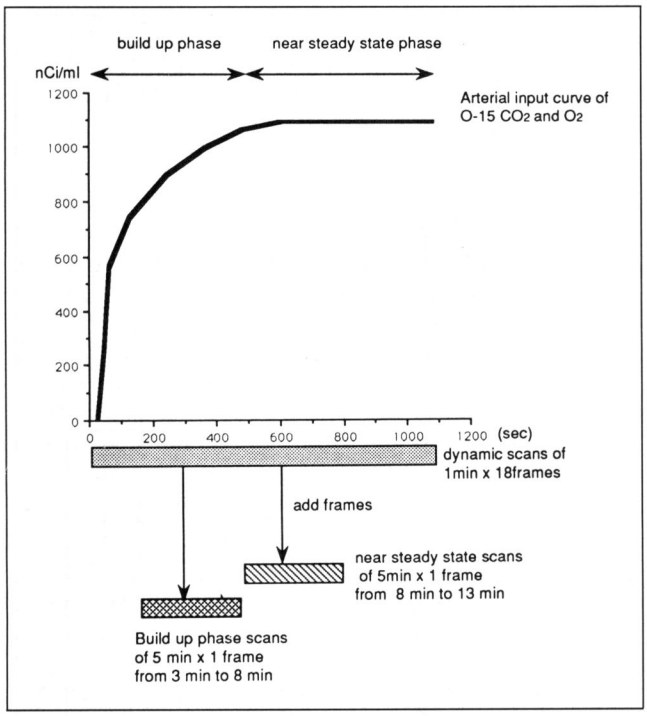

FIGURE 1. Scan and reconstruction protocol for build-up method.

averaged arterial activities were used. For the new method, both late build-up and near steady-state phase images were used to evaluate the time dependency of the calculated parameters.

Data Analysis

Profiles of Input Functions. To assess the profile of the input functions $C_a(t)$, $C_O(t)$ and $C_H(t)$ from the eight patients, each arterial input function was normalized with the mean arterial concentration of the presumed steady-state phase (10–18 min). The mean and standard deviation of eight curves were plotted at each measurement point (Fig. 2).

Simulation Study. A simulation study was performed with typical arterial input functions approximated by the exponential equations:

$$C_a(t) = 1067(1 - \exp[-t/110]),$$

$$C_O(t) = 1250(1 - \exp[-t/50]),$$

$$C_H(t) = 400(1 - \exp[-t/200]).$$

The weight contribution of the early build-up phase on the calculated parameters was assessed. In the $C^{15}O_2$ inhalation study, if $u < t$, the weight contribution of $C_a(u)$ from $u = 0$ to t_a on PET value T is a function of t_a:

$$h(t_a) = \frac{\int_{t_1}^{t_2}\int_{0}^{t_a} C_a(u)e^{-k_2(t-u)}\,du\,dt}{\int_{t_1}^{t_2}\int_{0}^{t} C_a(u)e^{-k_2(t-u)}\,du\,dt}.$$

If $h(t_a)$ is sufficiently small, the influence of $C_a(t)$ ($t = 0$ to t_a) on the PET value can be ignored. The weight contribution of $C_O(t)$ on C_2 and $C_H(t)$ on C_3 was also evaluated.

The effect of the delay and dispersion of the input function was evaluated. The measured arterial radioactivity is delayed and dispersed with respect to the cerebral arterial activity (*11,14*). The effect on the calculated CBF was estimated using the following equation. The measured input function $C_a(t)$ is expressed with the true input function $C_a^0(t)$ as:

$$C_a(t + d)e^{\lambda d} = C_a^0(t) * \left(\frac{e^{-\left(\frac{1}{\tau}+\lambda\right)\tau}}{\tau}\right),$$

where the dispersion function is assumed as $\frac{1}{\tau}\exp\left[\frac{-t}{\tau}\right]$ (*11,14*), and d is delay of the measured arterial curve. True tissue activity $C_T(t)$ and PET value T are expressed as:

$$C_T(t) = FC_a(t + d)\exp[\lambda d]\tau + FC_a(t + d) \cdot \exp[\lambda d](1 - \tau F/p) * \exp[-(F/p + \lambda)t]$$

$$T = \frac{1}{t_2 - t_1}\int_{t_1}^{t_2} C_T(t)\,dt.$$

When d and τ are known, the unique flow F can be calculated by the lookup table method:

$$F = G_{d,\tau}(T),$$

where $G_{d,\tau}(T)$ is a lookup table with the correction for delay and dispersion. As our method assumes both d and τ as null, percent error of calculated flow due to delay and dispersion is estimated as:

$$\%\text{ error in flow} = \frac{G_{0,0}(G_{d,\tau}^{-1}(F)) - F}{F} \times 100.$$

The same evaluation was performed on the conventional steady-state method. In the case of the constant input function,

$$C_a(t) = C_a,\ C_a^0(t) = C_a^0,$$

$$C_a^0 = e^{\lambda d}(1 + \lambda\tau)C_a.$$

Measured CBF F_d and true CBF F are:

$$F_d = \frac{\lambda}{\frac{C_a}{C_T} - 1},$$

$$F = \frac{\lambda}{e^{\lambda d}(1 + \lambda\tau)\frac{C_a}{C_T} - 1},$$

$$\%\text{ error in flow} = \frac{F_d - F}{F} \times 100 = \left(\frac{\frac{\lambda}{e^{-\lambda d}(F + \lambda)}}{(1 + \lambda\tau)} - 1 - F\right) \times 100.$$

The effect of tissue heterogeneity on CBF measurement was assessed with the late build-up phase and the steady-state phases. Error in measured flow was calculated for a region of interest (ROI) containing varying proportions of two tissues with equal partition coefficients of 1 ml/g, but with different flows, assuming

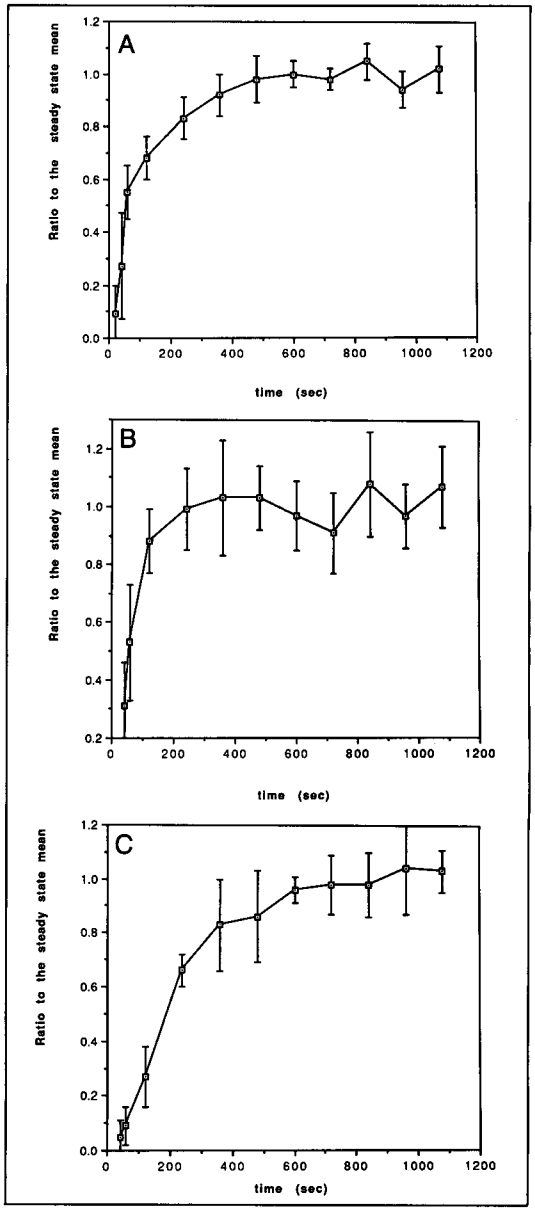

FIGURE 2. Mean arterial input functions of eight patients in CBF study using (A) $C^{15}O_2$ inhalation for $C_a(t)$ and (B) $^{15}O_2$ inhalation for $C_O(t)$ and (C) $C_H(t)$. Each arterial input function was normalized with the mean value of steady state, that is, from 10 to 18 min. Mean ± s.d. was plotted at each time point of measurement.

20 ml/min/100 g for white matter and 80 ml/min/100 g for gray matter. Percent underestimation was calculated with the following equation:

$$\% \text{ underestimation} = \frac{g\alpha + w(1-\alpha) - G(G^{-1}(g)\alpha + G^{-1}(w)(1-\alpha))}{g\alpha + w(1-\alpha)} \times 100,$$

where G is a lookup table from tissue activity to flow, g is the CBF value of gray matter, w is the CBF value of white matter and α is the proportion of gray matter in a ROI.

The statistical noise of CBF images obtained with the new method was compared between the build-up phase and the near steady-state phase. In the latter phase, there was a tradeoff between better count statistics and more noise propagation due to a larger nonlinearity in the count-flow relationship. The statistical error in CBF(ΔCBF/CBF) was estimated as:

$$\frac{\Delta CBF}{CBF} = \frac{\frac{\partial f}{\partial T}}{\frac{f}{T}} \frac{\Delta T}{T},$$

where $\frac{\partial f}{\partial T}$ is the slope of the lookup table (*18*). The term $\frac{\partial f/\partial T}{f/T}$ is an error propagation factor from tissue count rate to flow, indicating nonlinearity in the count-flow relationship. The statistical noise of the integration (ΔT) was estimated using the statistical relationship $\Delta T \propto \sqrt{T}$ (*18*).

Validation Study. With the data obtained from the eight patients, CBF and OEF images were calculated with the conventional steady-state method and the new method. The new method was applied to both the late build-up phase and the near-steady-state phase. The conventional steady-state method was applied to the near steady-state phase. Whole brain ROIs were taken in the

TABLE 1
Percent Weight Contribution of Early Build-up Phase (t = 0 to t_a) of $C_a(t)$, $C_O(t)$ and $C_H(t)$ on the Calculated Parameters T, C_2, and C_3 Obtained from the Late Build-up Phase (3–8 min)*

	Phase (t = 0 to t_a)		
	0–60 sec	0–120 sec	0–180 sec
$C_a(t)$ on T	0.8	4.9	16.6
$C_O(t)$ on C2	1.2	6.4	19.8
$C_H(t)$ on C3	0.6	3.7	14.2

*F = 50 ml/min/100 g.

slices 84 mm above the orbitomeatal line, including the centrum semiovale, to analyze systematic differences in the calculations. ROIs were defined in $C^{15}O_2$ tissue activity images of the near steady-state and projected on the parametric images. When the slices showed infarction, slices from the normal hemisphere were used.

RESULTS

Profiles of Input Function

During $C^{15}O_2$ inhalation, arterial radiotracer activity rose steeply during the first minute, gradually increased from 1 to 8 min, and reached steady-state at approximately 8 min. During $^{15}O_2$ inhalation, the arterial concentration of $^{15}O_2$ rose rapidly during the first 2 min and reached steady-state at approximately 4 min, although fluctuation of ±10% was observed during the later phase. The concentration of $H_2{}^{15}O$ gradually increased during the first 10 min and reached steady-state later (Fig. 2).

Simulation Study of Parameter Calculation

Weight Contribution of Early Build-up Phase. Table 1 shows the weight contribution of the early build-up phase on the input functions on T, C_2 and C_3 when the scans were performed at the late build-up phase. The weight contribution of the first minute was as small as 1%.

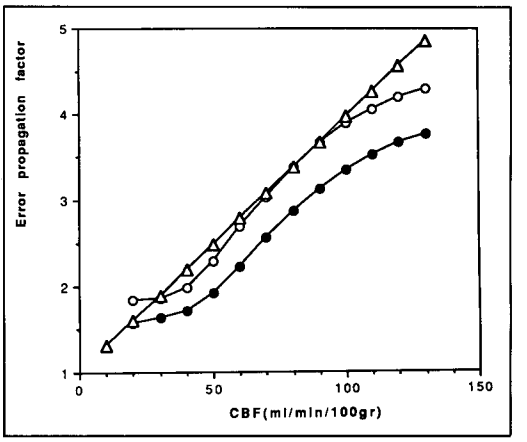

FIGURE 3. Error propagation factors from measured tissue activity to rCBF by the autoradiographic method with early build-up phase (closed circles) and with near steady-state phase (open circles) and by the conventional steady-state method (open triangles). Error propagation factor is systematically smaller in the autoradiographic method with early build-up phase (3–8 min) than in the conventional steady-state method. In the steady-state phase (8–13 min), both methods show almost equivalent error propagation in the range of 20 to 100 ml/min/100 g.

Delay and Dispersion Effect. Delay and dispersion effects on CBF were equivalent between the methods (Table 2). When the delay was 5 sec, overestimation of the calculated CBF at 50 ml/min/100 g was approximately 7%. A 5-sec delay was equivalent to a 2.5-sec delay plus a 2.5-sec dispersion (Table 2).

Tissue Heterogeneity Effect. Figure 3 shows error propagation factors plotted against CBF. Nonlinearity between flow and tissue activity is most prominent in the conventional steady-state method, less prominent in the autoradiographic method at near steady-state and least prominent in the autoradiographic method at the late build-up phase.

Figure 4 shows the tissue heterogeneity effect on CBF by the autoradiographic method with different scanning periods. Underestimation of CBF was less prominent with

TABLE 2
Percent Overestimation of CBF Due to Delay and Dispersion of Ca(t)

	CBF (ml/min/100 g)	Autoradiographic build-up method			Conventional steady-state method
		3–8 min	8–13 min	13–18 min	
Delay (3 sec)	30	4.5	3.9	4.2	3.3
	50	3.7	3.9	4.1	4.3
	80	5.9	5.4	5.1	6.0
Delay (5 sec)	30	6.8	6.8	6.0	5.5
	50	6.9	7.1	7.1	7.4
	80	10.2	9.7	9.6	10.3
Delay (2.5 sec and dispersion 2.5 sec)	30	6.8	6.0	6.3	5.5
	50	6.8	7.1	7.3	7.4
	80	10.1	9.6	9.3	10.3
Dispersion (5 sec)	30	6.8	6.0	6.2	5.5
	50	6.8	7.0	7.2	7.3
	80	10.1	9.4	9.2	10.2

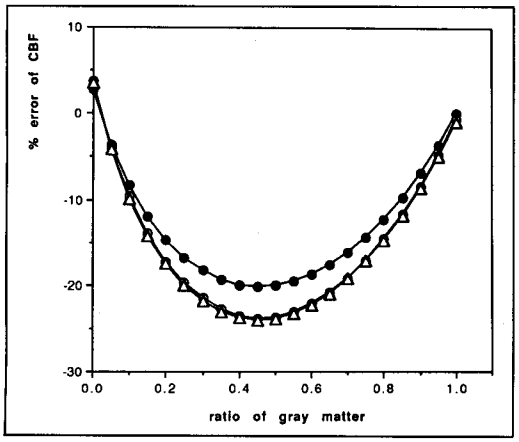

FIGURE 4. Effect of flow heterogeneity on CBF measurement by the autoradiographic method with early build-up phase (closed circles) and with near steady-state phase (open circles) and by the conventional steady-state method (open triangles). Error in measured flow was calculated for a ROI containing varying proportions of two tissues with different flows, that is, 80 ml/min/100 g for gray matter and 20 ml/min/100 g for white matter. The partition coefficient was fixed to unity. Note that systematic underestimation of CBF is smaller in the late build-up phase than in the steady-state phase.

the late build-up phase (3–8-min scan) than with the steady-state phase (8–13-min scan and 13–18-min scan). The tissue heterogeneity effect was equivalent with the conventional steady-state method and the autoradiographic method when the same scanning period (8–13 min) was used.

Statistical Errors of CBF. Statistical errors of CBF, ΔCBF/CBF calculated with the build-up method using the late build-up phase and the near steady-state phase were equivalent (Table 3).

Validation Study

Table 4 shows the comparison between the new method and the conventional steady-state method in eight patients. Because the whole brain contains a mixture of gray matter, white matter, cerebrospinal fluid and possibly lesions, the differences in the parameter estimates between the two methods indicate the overall effect by the autoradiographic method (*2*). Time dependency of CBF values was observed ($p < 0.01$, ANOVA). CBF values calculated with the late build-up phase were 11% higher than those with the near steady-state phase (8–13 min). CBF values calculated with the near steady-state phase in the build-up method were 2% higher than those with the conventional steady-state method, but the difference was not significant. No time dependency of OEF values was observed ($p > 0.8$, ANOVA). OEF values calculated with the build-up method and the conventional steady-state method were equivalent.

TABLE 3
Statistical Noise of CBF Images

CBF (ml/min/100 g)	ΔCBF/CBF	
	Late build-up (3–8 min)	Near steady-state (8–13 min)
20	0.00054	0.00048
50	0.00089	0.00101
80	0.00106	0.00114

ΔCBF/CBF was calculated with the relationship: $\Delta T = k\sqrt{T}$ $\frac{\Delta F}{F} = k\frac{EP(F)}{\sqrt{G^{-1}(F)}}$, where F is CBF, EP(F) is the error propagation factor at F, and G is lookup table from tissue activity to flow. Constant k was omitted in the table.

TABLE 4
In Vivo Comparison of the Calculated Parameters for the New Method with Late Build-up Phase (3–8 min) and Near Steady-State Phase (8–13 min) and the Conventional Steady-State Method

	Steady-state method	Autoradiographic method	
		(3–8 min)	(8–13 min)
CBF (ml/min/100 g)	33.7 ± 12.3	36.6 ± 11.1*	33.8 ± 11.5
OEF	0.455 ± 0.102	0.445 ± 0.077	0.440 ± 0.082
$CMRO_2$ (ml/100 ml/100 g)	2.68 ± 0.97	2.92 ± 0.80	2.69 ± 0.86

Values are mean ± s.d. (n = 8).
*$p < 0.01$ (ANOVA) for comparison with conventional steady-state method and near steady state phase of new method.

DISCUSSION

Our method is categorized as an autoradiographic method with ramped input function. Iida et al. (*18*) performed a systematic study of the shape of the input function and the duration of the scan in the autoradiographic method for CBF measurement. The bolus method, with sharp peaks and short scanning duration, is sensitive to delay and dispersion, but provides a linear count-flow relationship with less tissue heterogeneity effect. Dead-time error and accidental coincidence could be a problem. Because of the short scanning period, the calculated CBF is likely to fluctuate. In contrast, the ramped input function allows a longer scan duration, resulting in less sensitivity to delay and dispersion, and a larger nonlinearity which causes more effect of tissue heterogeneity. There is no dead-time problem. By administering sufficient amounts of $H_2{}^{15}O$ and scanning for a long period, the statistical error in CBF may be negligible. The contribution weights cover the whole scan period, providing more stable CBF values (*18*).

To apply the autoradiographic method to the build-up phase, preserving the simplicity of the conventional steady-state method, we first analyzed the profiles of input function to determine the optimal scan period. $C_a(t)$ and $C_O(t)$ showed a rapid rise in the first 2 min, later forming a gradual build-up phase. $C_H(t)$ showed a gradual increase in the first 10 min, while the absolute value was relatively small. Rapid change of or low radiotracer concentration in whole blood or plasma during the earlier build-up phase could cause measurement error. Additionally, in the gas

inhalation study, the respiratory cycle may cause variation in the tissue as well as arterial activity, particularly in elderly and diseased populations (*2*). These factors are accentuated with intermittent arterial sampling because of the limited sampling interval. For these reasons, the early build-up phase is not suitable for the scanning period.

The tissue radiotracer concentration is determined not only by the current arterial concentration but also by its weighted integral (convolution) during the preceding several minutes, unless steady state is achieved and maintained (*2*). When the late build-up phase (3–8 min) is adopted for the scanning period, calculated parameters of T, C_2 and C_3 are minimally affected by the input functions of the first 1–2 min. Intermittent blood sampling at intervals of 1–2 min would be sufficient because $C_a(t)$ and $C_O(t)$ rise steeply in the first 1–2 min, but decrease later (Fig. 2). Input functions would then be interpolated, assuming tissue radiotracer concentration at $t = 0$ is 0.

Correction of delay and dispersion of arterial input function is essential for accurate estimation of CBF (*11,14,18*). In this study, however, the correction was not performed for the following reasons. First, we adopted manual arterial sampling, in which external delay and dispersion were negligible. Second, it is impossible to measure the internal delay time and dispersion constant with the single-frame autoradiographic method. With the dynamic method, mean internal dispersion time is estimated at 5 sec if blood is sampled at the radial artery (*14*), and differences of arrival time ("head-to-hand" time lag) are 3 sec (*19*). However, the correction is not practical, as internal delay and dispersion depend on the site of arterial sampling (radial artery versus brachial artery) and on the location of the brain region (*20*). Third, the steady-state method is also subject to a delay and dispersion effect because of the short half-life of ^{15}O ($T_{1/2}$ = 123 sec). A 5-sec delay of arterial input function causes approximately a 3% decrease of the radiotracer activity, resulting in 7.4% overestimation of CBF at 50 ml/min/100 g. This overestimation has not usually been corrected (*1*). Lastly, as shown in Table 2, the delay and dispersion effect in the late build-up phase was as small as that in the near steady-state phase (8–13 min) and in the later steady-state phase (13–18 min) with the same scan duration.

The limited resolution of the PET scanner and the nonlinear count-flow relationship (Fig. 3) cause systematic underestimation of CBF (*21*). With the build-up method, the underestimation of CBF because of flow heterogeneity was larger in the near steady-state phase than in the late build-up phase (Fig. 4). In this study, the heterogeneity of the partition coefficient was not considered, because the autoradiographic method was designed to improve the conventional steady-state method which usually uses the fixed value of partition coefficient of water (*1,2*).

As shown in Table 4, CBF values calculated with the build-up method using the late build-up phase were higher than those using the near steady-state phase. This time dependency of CBF is caused by delay and dispersion of the input function, as well as by the tissue heterogeneity effect (*12,14*). As the former factor has the same effect in both the late build-up phase and the steady-state phase (Table 2), the tissue heterogeneity effect would be the main cause. Considering the diseases and older ages of our subjects, the effect of nonperfusable space might be large. In contrast, our method provided OEF values equivalent to those with the conventional steady-state method without time dependency. As expected from Equation 15 in the Appendix, OEF is mainly determined as the ratio of $\hat{C}_t$ and C_2, where time dependency might be canceled out.

In conclusion, our method is a simple and practical alternative to the conventional steady-state method for obtaining images of oxygen metabolism.

APPENDIX

The algorithm of the new method was presented by Senda et al. (*2*).

CBF Measurement with $C^{15}O_2$ Inhalation

CBF measurement was performed with an adaptation of Kety's diffusible autoradiographic method (*8*). The regional change in cerebral radiotracer concentration during $C^{15}O_2$ inhalation is described as:

$$\frac{dC_T(t)}{dt} = FC_a(t) - \frac{FC_T(t)}{p} - \lambda C_T(t) = FC_a(t) - \left(\frac{F}{p} + \lambda\right)C_T(t), \quad \text{Eq. 1}$$

where $C_T(t)$ is the tissue concentration of $H_2{}^{15}O$, $C_a(t)$ is the arterial concentration of $H_2{}^{15}O$ measured by blood sampling, F is the regional blood flow, p is the partition coefficient of water between brain and blood and λ is the physical decay constant of ^{15}O.

In steady-state, where $dC_T(t)/dt = 0$,

$$F = \frac{\lambda}{\frac{C_a}{C_T} + \frac{1}{p}}. \quad \text{Eq. 2}$$

In this method, $C_T(t)$ and $C_a(t)$ need not be constant:

$$C_T(t) = k_1 C_a(t) * e^{-k_2 t} \quad \text{Eq. 3}$$

where * indicates convolution,

$$k_1 = F,$$

$$k_2 = \frac{F}{p} + \lambda,$$

assuming $C_T(t) = 0$.

PET value T obtained from the scan from t_1 to t_2 is,

$$T = \frac{1}{t_2 - t_1}\int_{t_1}^{t_2} C_T(t)\,dt. \quad \text{Eq. 4}$$

The arterial activity curve $C_a(t)$ is determined by multiple blood sampling starting from the commencement of inhalation with interpolation between measured points to create a smooth curve. A lookup table, $F = G(T)$, is then generated to relate T to F, from which CBF is estimated.

OEF Measurement with $^{15}O_2$ Inhalation

Tissue radiotracer concentration $C_T(t)$ is the sum of tissue activity in proper $C_t(t)$ and blood-pool activity $C_b(t)$:

$$C_T(t) = C_t(t) + C_b(t) \qquad \text{Eq. 5}$$

The regional change in cerebral parenchymal radiotracer concentration during $^{15}O_2$ inhalation is:

$$\frac{dC_t(t)}{dt} = FEC_O(t) + FC_H(t) - \frac{FC_t(t)}{p} - \lambda C_t(t)$$

$$= FEC_O(t) + FC_H(t) - \left(\frac{F}{p} + \lambda\right)C_t(t), \qquad \text{Eq. 6}$$

where E is OEF, $C_O(t)$ is the arterial concentration of $^{15}O_2$ and $C_H(t)$ is the arterial concentration of $H_2{}^{15}O$ calculated from the activity of whole blood and plasma with $C^{15}O_2$ and $^{15}O_2$ inhalation, assuming that all the activity in the plasma comes from $H_2{}^{15}O$ (*2*).

$$C_H(t) = AC_P(t), \qquad \text{Eq. 7}$$

where A = (water content of whole blood)/(water content of plasma) and $C_P(t)$ is $H_2{}^{15}O$ activity in plasma.

Constant A can be derived if the packed cell volume (PCV) of the arterial blood is measured and the ratio of water between red cells and plasma is assumed constant (*1*).

$$A = 1 - 0.245\ PCV$$

$$C_O(t) = C_A(t) - C_H(t), \qquad \text{Eq. 8}$$

where $C_A(t)$ is ^{15}O activity in whole blood.

$$C_t(t) = (FEC_O(t) + FC_H(t)) * e^{-k_2 t}, \qquad \text{Eq. 9}$$

where $k_2 = \frac{F}{p} + \lambda$.

The regional radiotracer concentration in the vascular component $C_b(t)$ is:

$$C_b(t) = V_b(1 - E)C_O(t), \qquad \text{Eq. 10}$$

where V_b is the fractional blood volume.

In the steady state, all variables are time-independent:

$$C_T = C_t + C_b$$

$$= \frac{FEC_O + FC_H}{\frac{F}{p} + \lambda} + V_b(1 - E)C_O \qquad \text{Eq. 11}$$

or

$$E = \frac{C_T\left(\frac{F}{p} + \lambda\right) - FC_H - V_bC_O\left(\frac{F}{p} + \lambda\right)}{pC_O - V_bC_O\left(\frac{F}{p} + \lambda\right)}. \qquad \text{Eq. 12}$$

In the new method,

$$C_T(t) = C_t(t) + C_b(t)$$

$$= (FEC_O(t) + FC_H(t)) * e^{-k_2 t} + V_b(1 - E)C_O(t)$$

$$= E(FC_O(t) * e^{-k_2 t} - V_bC_O(t))$$

$$+ FC_H(t) * e^{-k_2 t} + V_bC_O(t). \qquad \text{Eq. 13}$$

PET value obtained from t_1 to t_2 is:

$$\hat{C}_T = \frac{1}{t_2 - t_1}\int_{t_1}^{t_2} C_T(t)\,dt$$

$$= \frac{1}{t_2 - t_1}\int_{t_1}^{t_2} \{E(FC_O(t) - V_bC_O(t))$$

$$+ FC_H(t)) * e^{-k_2 t} + V_bC_O(t)\}\,dt$$

$$E = \frac{-\int_{t_1}^{t_2}\{FC_H(t) * e^{-k_2 t} + V_bC_O(t)\}\,dt + (t_2 - t_1)\hat{C}_T}{\int_{t_1}^{t_2}\{FC_O(t) * e^{-k_2 t} - V_bC_O(t)\}\,dt}. \qquad \text{Eq. 14}$$

Or,

$$E = \frac{\hat{C}_T - (C_1 + C_3)}{C_2 - C_1} \qquad \text{Eq. 15}$$

where

$$C_1 = \frac{1}{t_2 - t_1}\int_{t_1}^{t_2} V_bC_O(t)\,dt \qquad \text{Eq. 16}$$

$$C_2 = \frac{1}{t_2 - t_1}\int_{t_1}^{t_2} FC_O(t) * e^{-k_2 t}\,dt \qquad \text{Eq. 17}$$

$$C_3 = \frac{1}{t_2 - t_1}\int_{t_1}^{t_2} FC_H(t) * e^{-k_2 t}\,dt. \qquad \text{Eq. 18}$$

The arterial blood is sampled several times during the study starting from t = 0 to obtain the $C_O(t)$ and $C_H(t)$.

ACKNOWLEDGMENT

The authors would like to thank Ms. B. J. Hessie for editorial assistance.

REFERENCES

1. Frackowiak RSJ, Lenzi G, Jones T, Heather JD. Quantitative measurement of regional cerebral blood flow and oxygen metabolism in man using ^{15}O and positron emission tomography: theory, procedure and normal values. *J Comput Assist Tomogr* 1980;4:727–736.
2. Senda M, Buxton RB, Alpert NM, et al. The ^{15}O steady state method: correction for variation in arterial concentration. *J Cereb Blood Flow Metab* 1988;8:681–690.
3. Lammertsma AA, Heather JD, Jones T, Frackowiak RSJ, Lenzi G. A statistical study of the steady state technique for measuring regional cerebral blood flow and oxygen utilisation using ^{15}O. *J Comput Assist Tomogr* 1982;6:566–573.
4. Jones SC, Greenberg JH, Reivich M. Error analysis for the determination of cerebral blood flow with the continuous inhalation of ^{15}O-labeled carbon dioxide and positron emission tomography. *J Comput Assist Tomogr* 1982; 6:116–124.
5. Correia JA, Alpert NM, Buxton RB, Ackerman RH. Analysis of some errors in the measurement of oxygen extraction and oxygen consumption by the equilibrium inhalation method. *J Cereb Blood Flow Metab* 1985;5:591–599.

6. Herscovitch P, Raichle ME. Effect of tissue heterogeneity on the measurement of cerebral blood flow with the equilibrium $C^{15}O_2$ inhalation technique. *J Cereb Blood Flow Metab* 1983;3:407–415.
7. Huang S, Mahoney DK, Phelps ME. Quantitation in positron emission tomography 8. Effects of nonlinear parameter estimation on functional images. *J Comput Assist Tomogr* 1987;11:314–325.
8. Kety SS. The theory and applications of the exchange of inert gas at the lungs and tissues. *Pharmacol Rev* 1951;3:1–41.
9. Raichle ME, Martin WRW, Herscovitch P, Mintun M, Markham J. Brain blood flow measured with intravenous $H_2{}^{15}O$. II. Implementation and validation. *J Nucl Med* 1983;24:790–798.
10. Mintun MA, Raichle ME, Martin WRW, Herscovitch P. Brain oxygen utilization with O-15 radiotracers and positron emission tomography. *J Nucl Med* 1984;25:177–187.
11. Lammertsma AA, Frackowiak RSJ, Hoffman JM, et al. The $C^{15}O_2$ build-up technique to measure regional cerebral blood flow and volume of distribution of water. *J Cereb Blood Flow Metab* 1989;9:461–470.
12. Lammertsma AA, Cunningham VJ, Deiber MP, et al. Combination of dynamic and integral methods for generating reproducible functional CBF images. *J Cereb Blood Flow Metab* 1990;10:675–686.
13. Lammertsma AA, Martin AJ, Friston KJ, Jones T. In vivo measurement of the volume of distribution of water in cerebral grey matter: effects on the calculation of regional cerebral blood flow. *J Cereb Blood Flow Metab* 1992;12:291–295.
14. Iida H, Kanno I, Miura S, Murakami M, Takahashi K, Uemura K. Error analysis of a quantitative cerebral blood flow measurement using $H_2{}^{15}O$ autoradiography and positron emission tomography, with respect to the dispersion of the input function. *J Cereb Blood Flow Metab* 1986;6:536–545.
15. Mukai T, Senda M, Yonekura Y, et al. System, design and performance of a newly developed high resolution PET scanner using double wobbling mode [Abstract]. *J Nucl Med* 1988;29:877.
16. Endo M, Hukuda H, Suhara T, et al. Design and performance of PCT-3600w (15-slice type): a whole-body positron emission tomograph [Abstract]. *J Nucl Med* 1991;32:1061.
17. Meyer E, Yamamoto YL. The requirement for constant arterial radioactivity in the $C^{15}O_2$ steady-state blood-flow model. *J Nucl Med* 1984;25:455–460.
18. Iida H, Kanno I, Miura S. Rapid measurement of cerebral blood flow with positron emission tomography. In: Chadwick DJ, Whelan J, eds. *1991 exploring brain functional anatomy with positron tomography*. Chichester: Wiley; 1991:23–42.
19. Dhawan V, Conti J, Mernyk M, Jarden JO, Rottenberg DA. Accuracy of PET rCBF measurements: effect of time shift between blood and brain radioactivity curves. *Phys Med Biol* 1986;31:507–514.
20. Iida H, Higano S, Tomura N, et al. Evaluation of regional differences of tracer appearance time in cerebral tissues using ^{15}O-water and dynamic positron emission tomography. *J Cereb Blood Flow Metab* 1988;8:285–288.
21. Iida H, Kanno I, Miura S, Murakami M, Takahashi K, Uemura K. A determination of the regional brain/blood partition coefficient of water using dynamic positron emission tomography. *J Cereb Blood Flow Metab* 1989; 9:874–885.